Energy 173 (2019) 75–91

Contents lists available at ScienceDirect

Energy

journal homepage: www.elsevier.com/locate/energy

Building heating and cooling load under different neighbourhood forms: Assessing the effect of external convective heat transfer

Pengyuan Shen [a, b, *], Mingkun Dai [c], Peng Xu [c], Wei Dong [d]

[a] School of Architecture, Harbin Institute of Technology, Shenzhen, 518055, China
[b] Urban Smart Energy Group, Shenzhen Key Laboratory of Urban Planning and Decision Making, Harbin Institute of Technology, Shenzhen, 518055, China
[c] School of Mechanical and Energy Engineering, Tongji University, Shanghai 201804, China
[d] School of Architecture, Harbin Institute of Technology, Harbin, 518055, China

ARTICLE INFO

Article history:
Received 28 September 2018
Received in revised form
5 February 2019
Accepted 8 February 2019
Available online 11 February 2019

Keywords:
Building simulation
Computational fluid dynamics
Heat transfer
Heating and cooling load
Neighbourhood design
Decision tree

ABSTRACT

Neighbourhood form imposes complex effects on the local microclimate. The overlook of neighbourhood microclimate will lead to miscalculation of building energy performance. In this paper, a neighbourhood-scale building simulation coupled between building energy simulation and CFD is proposed to assess the impact of external convective heat transfer coefficient (CHTC) to the building thermal performance. The co-simulation is run for different types of buildings inside the neighbourhood with different combinations of neighbourhood form parameters. The developed simulation scheme allows the iterations of neighbourhood design parameters and simulation model generation in CFD and EnergyPlus. Five empirical methods are used to predict CHTC, and the results of CHTC values, heating and cooling load intensity are compared in detail with the proposed CFD coupled method. The results suggest that the orientation and multiplier are crucial to the building load intensity in Chicago and the neighbourhood form can affect the thermal load of residential building up to about +27.1% and −18.6%, and +17.2% and −7.7% for office buildings. The proposed method and framework in this paper is capable of generating design guidelines for the optimal energy performance of the buildings in the neighbourhood.

1. Introduction

There are various factors affecting building energy use: environmental factors like the climate and weather conditions the building is situated in, building-wise factors such as the thermophysical properties of building envelopes, the shape of the building, the type of use, and the efficiency of the building systems, and etc. Urban areas are mainly made up of many building blocks with various set ups. The differences in geometry and orientation of the building blocks lead to different microclimate conditions, and they can affect the airflow around buildings. There are certain researches verifying the impacts of surrounding building arrays on the wind environment of specific buildings. Wind tunnels are used to investigate the wind pressure forces on buildings with different set ups of surrounding buildings by Lee et al. [1,2], and it is also used to understand the wind pressure distributions over a residential house by Bauman et al. [3]. Shishegar [4], Eliasson [5], Santamouris et al. [6] studied the air flows, natural ventilation conditions in urban canyons, and found wind sheltering effect in urban areas. Rubina et al. [7], demonstrated the urban wind climate is crucial in evaluating how much energy is being transferred between the outside air and the exterior surface of the building. There are also researches using CFD coupled method to study the local heat island problems in urban area [8] and the impacts of building height topology and buoyancy on local urban microclimates [9]. The simulation tool ESP-r also attempts to couple the CFD simulation to replace the traditional zonal network method and understand the building performance considering internal air flow [10–12].

In more recent studies, researcher began to pay attention to the influence of wind environment on building external CHTCs and building energy performance. Since building interacts with the atmosphere through convective heat transfer, and the convective heat transfer coefficient (CHTC) is an important factor in quantifying how much energy is being transferred between the outside air and the exterior surface of the building. The heat transfer created by convective heat transfer for a building wall is defined as follows:

$$Q_c = h_c A\left(T_{surf} - T_{wind}\right) \quad (1)$$

* Corresponding author. School of Architecture, Harbin Institute of Technology, Shenzhen, 518055, China.
E-mail address: Pengyuan_pub@163.com (P. Shen).

https://doi.org/10.1016/j.energy.2019.02.062
0360-5442/

Nomenclature:

a	Coefficient of terrain roughness
A	Surface area (m^2)
CLI	Cooling load intensity (W/m^2)
δ	Coefficient of terrain roughness
ΔT	Temperature difference ($^\circ C$)
h_c	Convective heat transfer coefficient (W/m^2K)
h_n	Heat transfer coefficient of natural ventilation (W/m^2K)
HLI	Heating load intensity (W/m^2)
LI	Load intensity (W/m^2)
R_f	Surface roughness multiplier
P	Perimeter (m)
Q_c	Convective heat transfer (W)
T_{air}	Temperature of local outside air temperature ($^\circ C$)
T_{so}	Temperature of outside surface ($^\circ C$)
T_{surf}	Temperature of building surface ($^\circ C$)
T_{wind}	Temperature of wind ($^\circ C$)
θ	Surface tilt angle (radius)
V_{ref}	Reference wind speed (m/s)
V_z	local wind speed calculated at the z (m) height above ground of the surface centroid (m/s)
W_f	Wind direction modifier
Z	Altitude (m)
Z_{ref}	Reference height (m)

Acronyms

ASHRAE	American Society of Heating, Refrigerating and Air-Conditioning Engineers
BCVTB	Building Control Virtual Test Bed
BES	Building energy simulation
CFD	Computational fluid dynamics
CHTC	Convective heat transfer coefficient
DOE	U.S. Department of Energy
DT	Decision tree
EUI	Energy use intensity
FAR	Floor area ratio
IDF	EnergyPlus input data file
MoWiTT	Mobile Window Thermal Test
NREL	National Renewable Energy Laboratory
SDF	Synchronous Data Flow
TARP	Thermal Analysis Research Program
TMY	Typical meteorological year
UDF	User defined function
XML	eXtensible Markup Language

where Q_c is the convective heat transfer in W, h_c is the CHTC in W/m^2K, A is the contact surface area in m^2, T_{surf} is the temperature of building surface, and T_{wind} is the temperature of the wind, in $^\circ C$. According to Equation (1), the convective heat transfer is proportional to the value of CHTC when the temperature of the surface and the wind are constant, which means it has direct impact on building energy transfer process. CHTC can be affected by the velocity and temperature of the wind that blows over the building surface. Studies have shown that the simulated energy consumption can vary up to 80% with different choices of CHTC calculation method for exterior surfaces [13]. Recently, computational fluid dynamics (CFD) has been used to assess the CHTC for building envelopes. CFD simulation has been proved to be a powerful tool with validated precision and is used to study the wind flow around buildings and its relationship with CHTC [14–19]. It is found that the use of CFD for the prediction of CHTC presents an increasing gain in accuracy over the recent years compared with empirical methods [20]. There are also researches trying to couple building energy simulation (BES) and CFD to provide more accurate estimations of CHTC values and building energy use [21,22]. However, most of the researches focused on problems of individual building immersed in an array of buildings. It is necessary to carry out a study which analyzes how neighbourhood form influences the energy performance of all buildings inside it by coupling CFD and BES, and find out how CHTCs calculated from different empirical methods and CFD will impact the building performance in terms of different building types in a neighbourhood.

2. Statement of objectives

As stated in the Introduction, the CHTC has great impact on the thermal performance of building and can be influenced by the wind environment of the local microclimate around the buildings. Therefore, a good estimation on CHTC values for the building envelope will be crucial to a valid BES. On the other side, the neighbourhood form will change the wind environment according to the literature research. Since there are few researches conducted to study the neighbourhood-scale energy performance with regard to the impacts from different CHTC calculation results and different neighbourhood forms, there is need in determining an efficient neighbourhood form to reduce the overall energy use of the buildings inside a neighbourhood. Therefore, in this research, two major tasks are going to be fulfilled:

1. Test different neighbourhood form and find its impact on the CHTC values as well as the energy performance of different types of buildings in the neighbourhood.
2. Use the CFD coupling method to estimate the external CHTCs of building envelopes in building performance simulation, and compare its results with empirical methods usually used in BES.

In this research, a neighbourhood is postulated to study the effect of wind environment on neighbourhood-scale building heating and cooling load in Chicago. The building types for the neighbourhood cover a variety of uses. Three controlling factors are chosen to describe the neighbourhood form, namely multiplier, orientation, and building setback of the neighbourhood, since wind environment will change according to the various combinations of these factors. The coupled simulation of BES and CFD is run for each combination of multiplier, orientation and setback. Five empirical methods usually used in EnergyPlus together with the CFD coupled method are used for the simulation, and their results of heating load intensity (HLI) and cooling load intensity (CLI) are compared. The proposed method and framework can be applied to the study in various places and climates. The simulation results and analysis aim to find a design guideline for the optimal overall energy performance of the buildings in the neighbourhood in Chicago.

3. Simulation framework

On coupling BES with CFD, there are many studies conducted on indoor environment in terms of CFD simulation for various research purposes including natural ventilation and indoor air quality [23–26]. In those studies, the simulation outputs from CFD, including air velocity, pressure, air temperature, etc., were used as the inputs for BES. Cezar [27] integrated BES and CFD to evaluate

Fig. 1. Scenarios of different multipliers.

the building energy consumption and indoor air quality. Srebric et al. [28] developed a coupled airflow-and-energy simulation program to calculate simultaneously the distributions of indoor airflow and thermal comfort and heating/cooling load. However, there are few research focusing on how the neighbourhood-scale microclimate is going to impact the energy performance of the buildings using coupled BES and CFD simulation though recently there is such attempt by using empirical methods [19]. One of the challenges is the difficulty and complexity in implementing the coupling between the two simulation engines for multiple buildings in a neighbourhood, especially when the coupling is dynamic.

3.1. Simulation scenario

3.1.1. Neighbourhood description

The postulated neighbourhood originated from a design project for a community in Chicago and the prototypical U.S. Department of Energy (DOE) reference buildings were used in this research to discuss the energy performance of the neighbourhood buildings. The neighbourhood was made up of six different types of buildings, including office building, residential building, school, supermarket, full restaurant, and quick restaurant (the full restaurant and the quick restaurant refer to the full-service restaurant and the quick-service restaurant defined by Commercial Prototype Building Models from DOE [29]). The numbers of each type of building in this neighbourhood were 6 for the residential, 4 for the full restaurant, 3 for the office, 2 for the quick restaurant, and 1 for the supermarket and the school. The office buildings and the residential buildings were set to be multi-floor buildings.

Three factors are considered in controlling the form of the neighbourhood in this research:

1) multiplier for multi-floor buildings

In order to control the density of the buildings in the area, multiplier for multi-floor buildings were used. Therefore, only two types of buildings — residential and office, were under the control of the multiplier. Different multipliers cause the buildings in the neighbourhood to be under different impacts of sunlight and wind. In this study, three multiplier values for the residential buildings were used: 5, 25, and 45, which means that the settings of 5 floors, 25 floors, and 45 floors were used for the residential buildings. For office buildings, the multipliers were 6, 32, and 58. An illustration of how multiplier affects the neighbourhood form is shown in Fig. 1.

2) Building orientation:

The orientation of each building is also an important factor that will change the microclimate of the neighbourhood regarding sunlight and wind environment. Eight orientations were concerned in this study. Relative to the north, the orientation degree varied from 0 to 360 with stepwise change of 45°. The orientation degree applied to all the buildings on the site.

3) Building setback:

Another factor that will change the density of a neighbourhood is the space between buildings, which is the building setback. Smaller setbacks among buildings will increase the neighbourhood density while larger setback decreases the density. There is research that studied the effect of the relationship between density and energy use intensity (EUI), concluding that the energy consumption decreases with increasing floor area ratio (FAR)[1] before FAR reaches a specific turning point, and then the relationship reverses [30]. However, the study did not take into account wind environment and detailed energy simulation. Five 5 setback values were used for the neighbourhood — 10, 20, 30, 40, and 50 m. Three examples of different setbacks among the buildings are shown in Fig. 2. The buildings in the neighbourhood were all coded with a name, starting from left to right and bottom to up and the original point of the coordinate system was the bottom left corner of “residential_0”. When orientation of the neighbourhood changes, the code name does not change with the orientation and still follows the naming rule that treats “residential_0” as the reference building.

3.1.2. The city of Chicago

In this research, Chicago is where the neighbourhood is situated. The city has a humid continental climate, which is categorized as Dfa in Köppen climate classification. The Typical Meteorological Year (TMY) weather data recorded from O'Hare International Airport is collected in from National Renewable Energy Laboratory (NREL) [31]. As shown in Fig. 3, the summer in Chicago could be hot with a July daily average of 24.3 °C, and exceeds 32 °C as many as about 20–30 days. In the winter, it could be cold and snowy, and the temperature can be as low as around −20 °C.

The average annual wind speed of Chicago is 16.6 km/h. Wind speed is a crucial factor in determining the outdoor thermal comfort as well as the feeling-like temperature in outdoor thermal condition. The winter in Chicago is already low in temperature, the outdoor thermal comfort condition would be even worsened when the low temperature is coupled with high wind speed. The TMY data indicate that most of the wind in Chicago during winter time comes from west or northwest, and the wind speed can be higher than 6 m/s. The maximum wind speed could be higher than 10 m/s.

3.2. Prototypical buildings

Six different types of buildings were included in this study as

[1] FAR: the ratio of total amount of usable floor area that a building has, or has been permitted to have, to the total area of the lot on which the building stands.

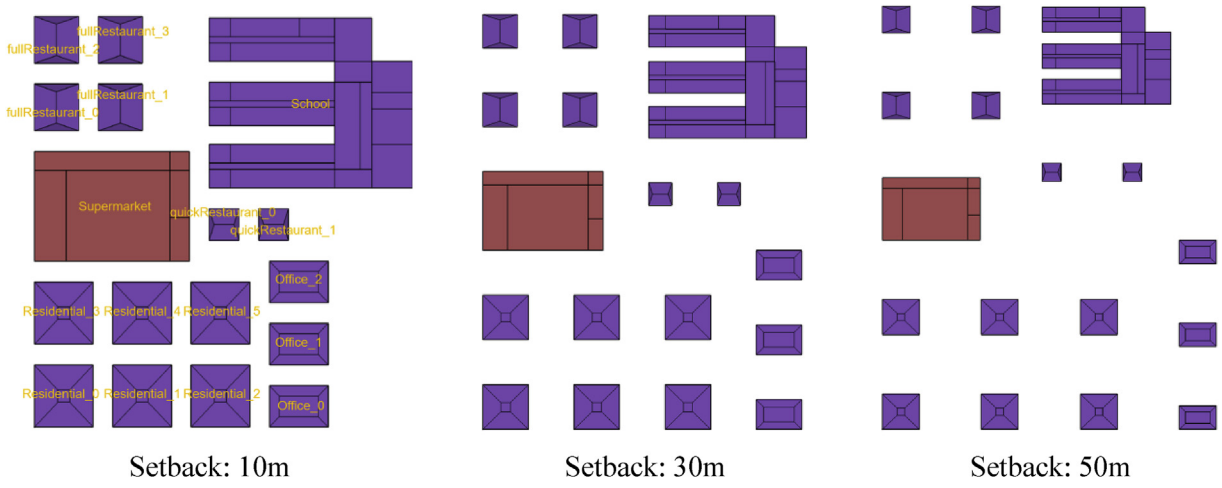

Fig. 2. Scenarios of different setbacks.

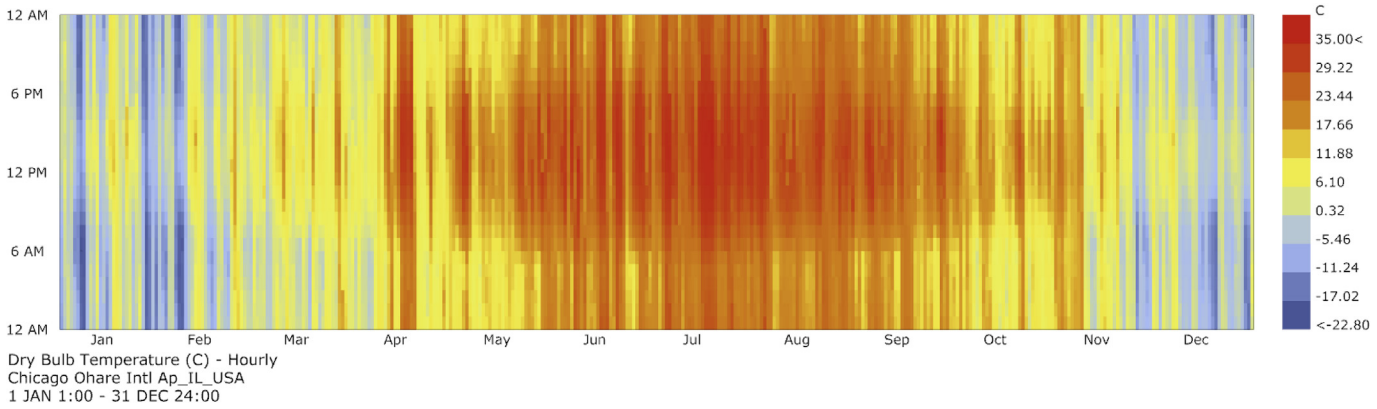

Fig. 3. Hourly temperature of TMY3 in Chicago.

indicated in Fig. 4. They were multi-floor residential, multi-floor office, full restaurant, quick restaurant, supermarket, and school. For restaurants, supermarket, and school, the commercial prototype building models for EnergyPlus developed by the DOE [32] were used and it was assumed that their number of floors did not change. These four types of buildings conform to the ASHRAE 90.1 2016 standard [33,34].

The office and residential buildings were developed to model how the height of tall buildings affected the energy use of the neighbourhood. The core-perimeter modeling method was used for the office building. The residential building has four units per floor. Five sets of multipliers were applied to the two types of buildings as described in 3.1.1.

3.3. Simulation run period

Though the BES is far less intensive in computational cost compared with CFD simulation, the coupled simulation process needs to have both of the two engines work together and it would be infeasible to do hourly simulation for a whole year. The goal of this research is to understand how the wind environment in winter Chicago is going to affect the building's thermal performance, choosing one specific day in the winter suffices the need of the task. Jan. 7th in the TMY is chosen as the day of interest since the coldest outdoor temperature occurs on that day and the wind direction is NW during most time of the day, which is a typical wind direction in Chicago during the winter.

The coupled simulation was run for a full day on Jan. 7th for each combination of multiplier, orientation, and setback. During the simulation of that day, the determination of simulation timestep in BES is important in deciding if the simulation is conducted too frequently or the produced simulation results are biased. In Ref. [35], it is suggested that after a certain sufficient time interval the accuracy will be the same even though the time step gets smaller in EnergyPlus. Zhai et al. found that normally a convergence can be reached after 4 to 10 iterations [23]. In the coupled simulation, the timestep of EnergyPlus simulation is set to be 4 steps an hour, which is 15 min, and it would be good enough to achieve converged EnergyPlus simulation results [21].

3.4. Simulation framework

3.4.1. Preprocessing of EnergyPlus input data files

To generate the neighbourhood based on the prototypical buildings in section 3.2, the original information of the six prototypes should be read and processed. A Python module was responsible for handling the information in the original EnergyPlus input data file (IDF) files of the buildings. Since the IDF format for EnergyPlus model was scripted in text form, it is not difficult to process the modeling information. The geometries of the prototypes were read in the following hierarchy: 1) building 2) surface 3) vertex. Additionally, the maximum value of vertex for each

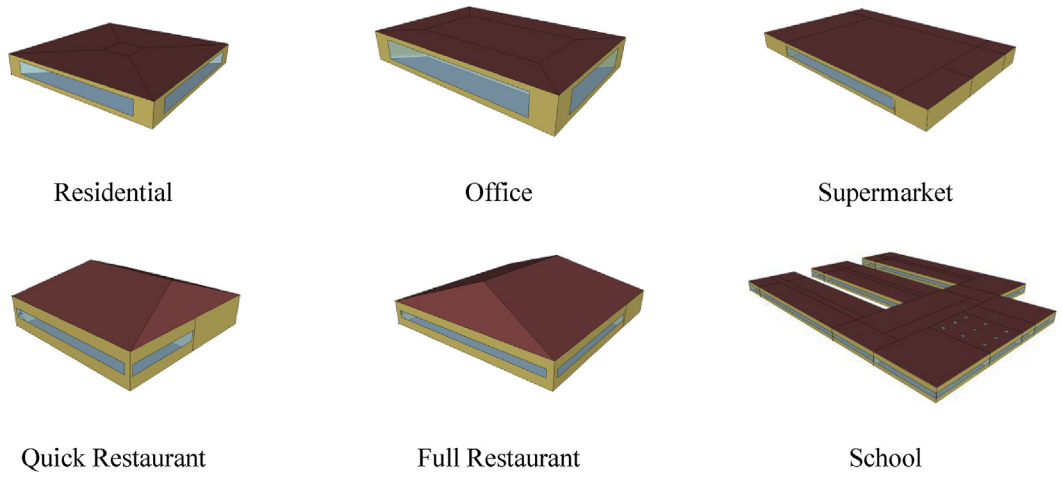

Fig. 4. Geometry of six prototypical buildings.

coordinate was also added into the dictionary as the length, width, and height information of the building.

After reading the information, some basic settings of the simulation in this research were also injected into the original IDFs, including: 1) simulation period: day Jan 7th; 2) simulation timestep: 15 min; 3) the output variables of the simulation; 4) multiplier value for the floor number of office and residential building according to the combination scenario.

3.4.2. Neighbourhood form

When the original geometric information was collected into a Python dictionary after preprocessing the IDF files of prototypical buildings, a full dictionary of altered geometries including all 17 buildings in the neighbourhood was generated based on the input vector of [multiplier, orientation, setback]. The full dictionary would take charge of the geometric manipulation in both generation of EnergyPlus models and meshing model for the buildings in the neighbourhood.

For EnergyPlus models, 17 building were needed to be modelled in total. As solar irradiation is one of the major factors driving thermal dynamic factors for buildings performance simulation [21], the model inputs for surrounding buildings who provide shading during the simulation period should be considered. To achieve this goal, the EnergyPlus models for the 17 buildings were created in turn. When one particular building was being modelled, the other building's geometric information was treated as the "Shading:Building:Detailed" object in EnergyPlus. Then during the simulation of that building, the solar irradiation hitting on the building facade, which is subject to the shading effect of surrounding buildings, was considered. In the meantime, the mesh file for the neighbourhood was also created in Gambit and exported to local folder in terms of the geometric information of the full dictionary.

3.5. Simulation by empirical methods

In EnergyPlus, there are several empirical methods being used in the building simulation for predicting CHTC value at each timestep given an outdoor environmental condition. In this research, besides using the proposed CFD coupled method to predict CHTC for the building, all the five empirical methods available in EnergyPlus are also used in BES, and the results of the proposed method and the empirical methods are compared regarding both CHTC and building heating and cooling load. The five empirical methods are DOE-2, SimpleCombined, TARP (Thermal Analysis Research Program), MoWiTT (Mobile Window Thermal Test), and AdaptiveConvection algorithm. The simulation using empirical methods are conducted following the same workflow as CFD coupled method, except that the coupled simulation procedure using BCVTB is skipped and the EnergyPlus runs on its own using all the CHTC calculation based on each empirical method.

A brief introduction of the empirical methods are given here [36]. The SimpleCombined algorithm uses surface roughness and local surface wind speed to calculate the exterior CHTC. The equation of calculating CHTC for SimpleCombined is [37]:

$$h_c = D + EV_z + FV_z^2 \tag{2}$$

where D, E, F are material roughness coefficients and V_z is the local wind speed calculated at the height above ground of the surface centroid. For example, a medium rough material like concrete has a coefficient of D, E, F as 10.79, 4.192, 0.0.

For the TARP algorithm, the equation is as follows [38]:

$$h_c = 2.573 W_f R_f \left(\frac{PV_z}{A}\right)^{0.5} + h_n \tag{3}$$

$$h_n = \begin{cases} \dfrac{9.482|\Delta T|^{\frac{1}{3}}}{7.283 - |\cos\theta|} & (\Delta T < 0 \text{ and upward facing or} \Delta T > 0 \text{ and downward facing}) \\ \dfrac{1.810|\Delta T|^{\frac{1}{3}}}{1.382 + |\cos\theta|} & (\Delta T < 0 \text{ and downward facing or} \Delta T > 0 \text{ and upward facing}) \end{cases} \quad \Delta T = T_{so} - T_{air} \tag{4}$$

where h_n is the heat transfer coefficient of natural convection; A, P are the surface area of the surface and perimeter of the surface in m^2 and m; R_f is the surface roughness multiplier, T_{air}, T_{so}, and ΔT are local outdoor air temperature calculated at the height above ground, outside surface temperature, and temperature difference between the surface and air, in $^\circ C$. W_f is wind direction modifier (1.0 when windward and 0.5 when leeward), and leeward is defined as greater than 100° from normal incidence of the wind; θ is the surface tilt angle.

The MoWiTT algorithm has the following form [39]:

$$h_c = \sqrt{\left[C_t \Delta T^{\frac{1}{3}}\right]^2 + \left[aV_z^b\right]^2} \tag{5}$$

where constant a, b, C_t are 3.26, 0.89, 0.84 when the surface is windward, and 3.55, 0.617, 0.84 when the surface is leeward.

The DOE-2 convection model is a combination of the MoWiTT and BLAST Detailed convection models, and is very similar to MoWiTT model. The calculation of CHTC for a smooth surface is described as:

$$h_{c,glass} = \sqrt{h_n^2 + \left[aV_z^b\right]^2} \tag{6}$$

where h_n can be calculated using Equation (4). For less smooth surface, the CHTC is modified according to Equation (7).

$$h_c = h_n + R_f\left(h_{c,glass} - h_n\right) \tag{7}$$

The AdaptiveConvection algorithm is a combination of separate model equation selections for h_n and h_f based on different surface classifications. The detailed descriptions of how each category of surfaces are treated can be found in Ref. [36] and they will not be introduced here. The major driving factors for AdaptiveConvection are still ΔT and V_z.

According to the different algorithms of empirical calculation methods, one of the most important driving factors of determining the value of CHTC is the wind speed. As introduced in the previous section, the simulation period for EnergyPlus is from 12 a.m., Jan 07–12 a.m., Jan 08. The timestep for the simulation is 4 times an hour, which is 15 min. The wind condition during the day in Chicago' TMY weather is plotted in Fig. 5. The wind speed ranges from 2 m/s to 6.5 m/s, which peaks at around 11 a.m. in the morning and falls to the valley in the night. The wind direction ranges from 280 to 350°, which are mostly northwesterly and northerly.

Since buildings are located in the troposphere where the wind speed increases with altitude, the wind velocity should be mapped by a function describing the relationship between wind speed and altitude. In ASHRAE Handbook of Fundamentals [40], the wind speed measured at a meteorological station is extrapolated to other altitudes according to Equation (8):

$$V_z = V_{ref}\left(\frac{\delta_{ref}}{Z_{ref}}\right)^{a_{ref}}\left(\frac{Z}{\delta}\right)^{a} \tag{8}$$

where, V_z is the wind speed at altitude z; V_{ref}, Z_{ref} are the reference wind speed and reference height, and they are referred to the data collected in the meteorological station who has a standard altitude of 10 m above the ground in an open field; a and δ are coefficients related with terrain roughness.

In Fig. 5, the wind speed profile in the area is plotted. The profile of three different speeds at the reference heights of 10 m are chosen to be presented: 2 m/s, 4 m/s, and 6 m/s. At the speed of 6 m/s, the wind velocity can reach 13 m/s at the height of around 185 m–190 m. For low speed wind at reference height, its value can also be double at the height of 190 m.

4. Coupling procedure

4.1. Coupling method and platform

There are basically two ways in doing coupling between BES and CFD when studying the impact of wind environment on building's surface or envelope as stated by Ref. [21]. One way is to integrate the simulation results of CFD in a one-level way by simply introducing the variables of interest from CFD to BES. Another way is called dynamic coupling, or sometimes referred as Ping-Pong coupling [23], in which the two simulation platform are constantly and regularly "talking" with each other, or, just like playing a Ping-Pong game, hitting the "ball" one at a time between each other. The only difference is that the "Ping-Pong ball" here refers to the information containing the variables of interest here in this research, which are obtained by running the simulations in the two platforms. A coordinator should be there, taking charge of understanding and handling the information from the two platforms and in the meantime, exchanging the information one at a time.

In this research, the tool that is playing the role of "coordinator", is called Building Control Virtual Test Bed (BCVTB), which was developed by Lawrence Berkeley National Laboratory (LBNL). The BCVTB is programmed on the basis of Ptolemy II software, which is a Java-based open-source software framework developed by the University of California at Berkeley to study modeling, simulation

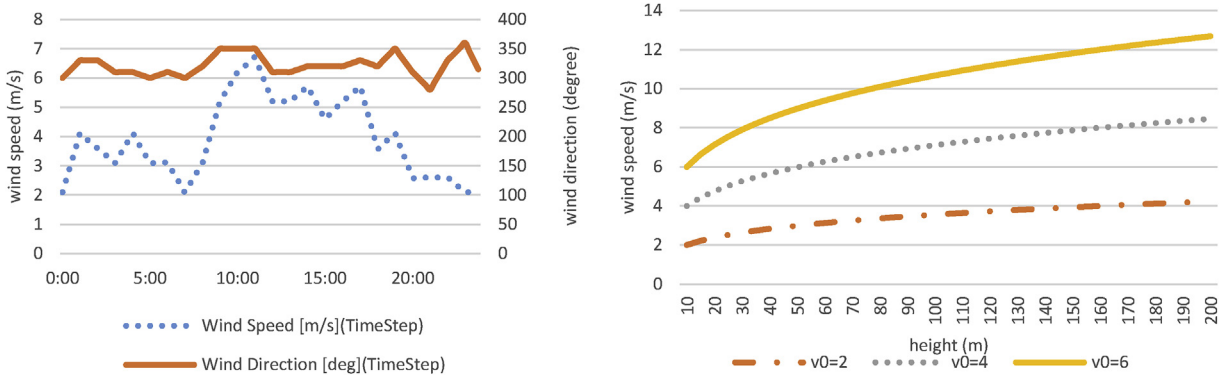

Fig. 5. Wind condition on Jan. 7 in TMY of Chicago and wind profile of height.

and design of concurrent heterogeneous real-time systems [41]. The reasons of using this tool are that the data transfer between simulation programs will be more computationally efficient than in the individual simulation programs when performing a co-simulation for a whole building and that it is developed in a modularized way and independent among simulation tools so that different clients can be coupled to it [42]. The latter reason means that not only those built-in simulation tools such as EnergyPlus, MATLAB, Simulink, Dymola can be coupled with each other, external simulation tools like Fluent can also be coupled. Though BCVTB does not have built-in functions for the coupling of CFD software, users are provided with freedom for tailor-made procedure that enables the coupling with self-developed program.

Fig. 6 shows the diagram of how the coupling is performed with BCVTB. The coupling mechanism in BCVTB can be described as follows: There are two clients - EnergyPlus and Fluent. Both of them are supposed to solve their own ordinary differential equation. Let's denote two functions f_f and f_e that compute the next value of state variables in Fluent and EnergyPlus, and they are executed with their respective code of sequence. f_f is provided with an initial value and f_e is coupled to the solution of f_f. Meanwhile, f_f is also coupled to the solution of f_e that has an initial value as well. Now let's denote the number of time steps as N and let $i \in \{0, \ldots, N\}$ be the time steps. f_f computes in its time step sequence $i \in \{0, \ldots, N-1\}$:

$$x_f(i+1) = f_f\left(x_f(i), x_e(i)\right)$$

And EnergyPlus computes the sequence

$$x_e(i+1) = f_e\left(x_e(i), x_f(i)\right)$$

With initial conditions $x_e(0) = x_{e,0}$ and $x_f(0) = x_{f,0}$. As noted by M. Wetter [42], there is an implementation difficulty in the situation that both f_f and f_e need to now the initial value of the other simulator, so at $i = 0$, both simulators exchange their initial value $x_{e,0}$ and $x_{f,0}$. During the time sequence of the two simulators, Fluent sends the new state $x_f(i+1)$ to the BCVTB and will not advance into the next time step until it receives the state $x_e(i+1)$ of EnergyPlus from the BCVTB. The same procedure also happens in EnergyPlus so that it does not matter which one of them is called in the first place.

4.2. Coupling variables

The concerned variables that participated in the exchange between EnergyPlus and Fluent include the CHTC variable from CFD, and exterior surface temperature, wind speed, wind direction, outdoor air temperature, current month, day, and hour from EnergyPlus. Since outdoor environmental variables from EnergyPlus need only to be exported once, setting one building in the neighbourhood to send this information to the BCVTB is sufficient.

The BCVTB was responsible for feeding the outdoor environmental variables like wind speed and surface temperature of EnergyPlus to Fluent as boundary condition for simulation, retrieving simulation results of CHTC from CFD and sending them back to EnergyPlus for building simulation until the time step of EnergyPlus reached the specified end of time flag. A texted based variable configuration file called “variable.cfg” was a key component in the coupling procedure because it contained all the variables participating in the exchange.

4.3. Setup of actuators in EnergyPlus

To implement an interface in EnergyPlus linked to BCVTB, a module called “ExternalInterface” were added in EnergyPlus starting from version 5.0. This interface is a series of objects that is in charge of receiving data from BCVTB, feeding it to EnergyPlus, then retrieving calculation results from EnergyPlus, and sending the required information to Fluent at each time step. These objects are granted the authority to overwrite certain EnergyPlus variables at each time step. In this research, ExternalInterface: Actuator was used to receive the simulation results of CHTC from BCVTB and overwrite the CHTC value for each surface of each building. For the actuator object, it is optional to set an initial value for it or if not specified, then the actuator only overwrites the actuated component after the warm-up and system sizing, which means that their

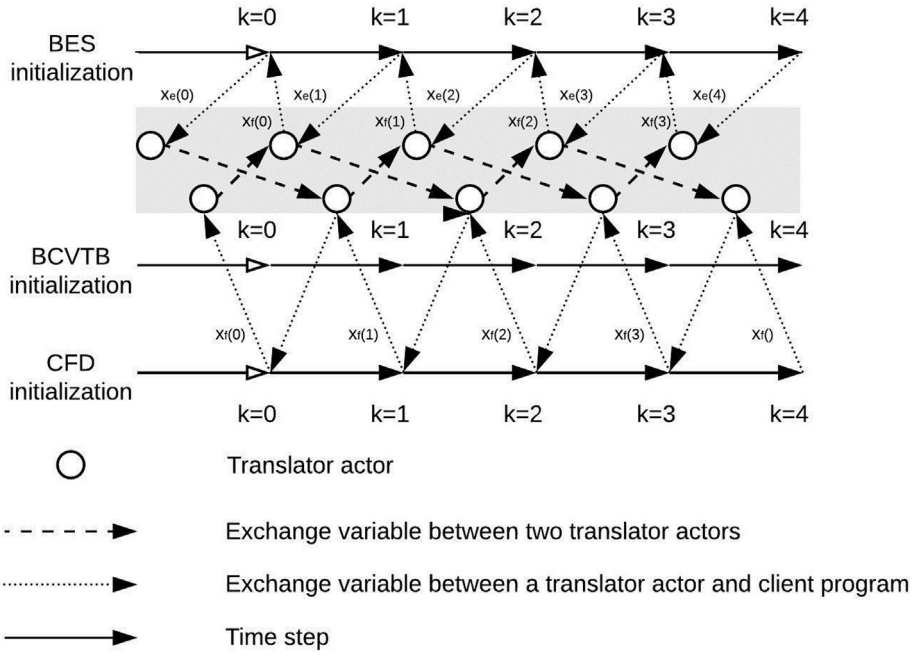

Fig. 6. Data synchronization and function calls between the translator and BES and CFD.

initial values can be defined during the warm-up and system sizing period in the simulation.

4.4. CFD model

Gambit was used to model the meshes according to the process described in 3.4.2. A Python script that is responsible for handling the neighbourhood geometry generated the Gambit journal file. This journal file was read by Gambit to finish the meshing of the CFD model and to export a meshing file that can be imported by Fluent. Then Fluent was called to run another journal file — the Fluent journal file, which was created by a programmed script and it is in this journal file that all the boundary conditions and the outputs information were provided.

The discretization method for the CFD simulation was finite element method. The standard k- ε turbulence model and the scalable wall function were used for the CFD simulation. The scalable wall function was used since it produces consistent results for grids of varying y+, and the y + values averaged around 120 for different cases in this study. Hexahedral meshing was used for the grid generation, and the grid got finer in the area of interest but grew coarser when distance from the area of interest increased. For example, for the grid generated for the CFD model of (25 multiplier, 225 orientation, 20 setback) combination, the mesh size on the building wall surface was 0.2 m. The generated grid owned good quality. The skewness value of grid for that case was 0.31 and the grid had around 2 million hexahedral cells in total.

In the Fluent journal file, the boundary conditions including wind speed, wind direction, wind temperature as well as the exterior wall temperature of each building were recorded. The wind direction in the CFD simulation was controlled by setting the boundaries of the outer box as different velocity-inlet. The wall surface temperature was set by the exterior wall temperature of each building imported from EnergyPlus at each timestep. At the end of the coupled step, the CHTC reader actor in the BCVTB model read the updated CHTC values resulted from CFD simulation and fed them to the EnergyPlus actor.

The simulation of the atmospheric boundary layer was achieved by taking advantage of the user defined function (UDF) that is coded in C programming language in Fluent. A UDF file named “udf.c” was created by Python scripting and the interpretation of wind velocity by altitude was provided for each velocity-inlet of the CFD model according to Equation (8). In regard to the computational heaviness of this research, the CFD simulation was conducted in parallel which makes use of all the CPUs of a 16-core workstation. 10^{-6} for energy equation, 10^{-4} for continuity, k and ε were used as the criteria for simulation convergence. The CFD simulation usually converged in about 400–800 iterations for different sets of boundary conditions.

5. Results and discussion

5.1. Results of CHTC by different algorithms

Considering that there are many buildings and their respective external surfaces involved, to visualize the results of CHTC for buildings in the neighbourhood obtained from different algorithms and the proposed CFD method, the CHTCs on all the surfaces of a particular building at each timestep were averaged and plotted as a heatmap. Representative heatmaps for each type of building are shown to analyze the CHTC calculation results of different algorithms:

In the heatmap, the x-axis represents the 24 h on Jan. 7th, and the y-axis contains the series number (from 1 to 120) of combinations made up of (multiplier, orientation, and setback) starting from (5, 0, 10) and ending with (45, 315, 50).

In Fig. 7, the average CHTC values of all building surfaces for a certain building is plotted. For the multi-floor building, residential_3, and office_1 are chosen to be the representatives. Residential_3 locates at the second row. Office buildings share same pattern in the CHTC results, therefore office_1, which locates in the middle, is chosen. For single-floor buildings, quick restaurants and full restaurants share similar patterns, so fullRestaurant_0 is chosen.

For the combinations on the y-axis, the multiplier grows from 5 to 45 every 40 series number. Therefore, for multi-floor buildings (residential and office), it can be observed that the average CHTC values simulated by various algorithms grow darker along y-axis, meaning the CHTC values increase when the building becomes higher. This is not surprising considering that when the height of the building increases, the velocity of the wind hitting the building surface becomes higher as shown in Fig. 5. Due to the fact that the CHTC is highly dependent on the wind speed no matter which algorithm is used for the calculation and that the CHTC increase correspondingly when velocity increases, this pattern can be straightforwardly explained. However, the magnitudes of the CHTC values differ among algorithms. The proposed CFD coupled simulation method has the highest CHTCs with an approximately maximum average value of 40 W/m^2K for the residential and office building. For empirical methods, SimpleCombined method has the biggest maximum average CHTC and the TARP method has the smallest because in SimpleCombined algorithm, the influence of wind speed variable on CHTC is big and follows a linear pattern, while in TARP algorithm, the influence of wind speed is diminished by the squared term. For other algorithms, most of the CHTC values fall between the values of SimpleCombined and the TARP method. The CHTC values calculated by empirical algorithms show a regular pattern, but the proposed CFD coupled method does not, which can be attributed to that the CFD method treat the buildings with more details and subtlety — the CHTC result of each surface of the building responds to the unique wind environment generated by the neighbourhood pattern and boundary conditions that are under the impact of various multiplier, orientation, setback, wind speed, wind direction, building surface temperature, and outdoor air temperature at each timestep.

The results of DOE-2 and MoWiTT are very close for all types of buildings because their algorithms are similar. The calculation results of SimpleCombined are identical among different combinations of orientations and setbacks because the algorithm does not take wind direction into account. For DOE-2, MoWiTT, TARP, and AdaptiveConvection algorithm, the wind directions relative to the building are considered, but only two conditions — windward and leeward are taken care of, except that in the AdaptiveConvection algorithm, one more situation is handled, which is that the roof surface is treated differently with building vertical surface such as wall and window. It is indicated that for most empirical algorithms (except for the SimpleCombined), the heatmap shows a plaid-like pattern along the y-axis. This is caused by that when the orientation of the building changes periodically (from 0° to 315°), the target building is treated either windward or leeward by the algorithm periodically, resulting in the plaid pattern. Using the CFD coupled method, the heatmap pattern becomes more complicated and irregular as it tries to decode the real-situation wind environment. When reading the heatmap from left to right for each algorithm, there are vertical white stripes being observed in the heatmap, which indicates low averaged CHTC values for all the buildings at those timesteps. The places where those white stripes occur agree with the low wind speed at the particular time, for example, 7 a.m. and the timesteps after 9 pm.

The most interesting difference between the results of the proposed CFD method and the empirical methods are for single-

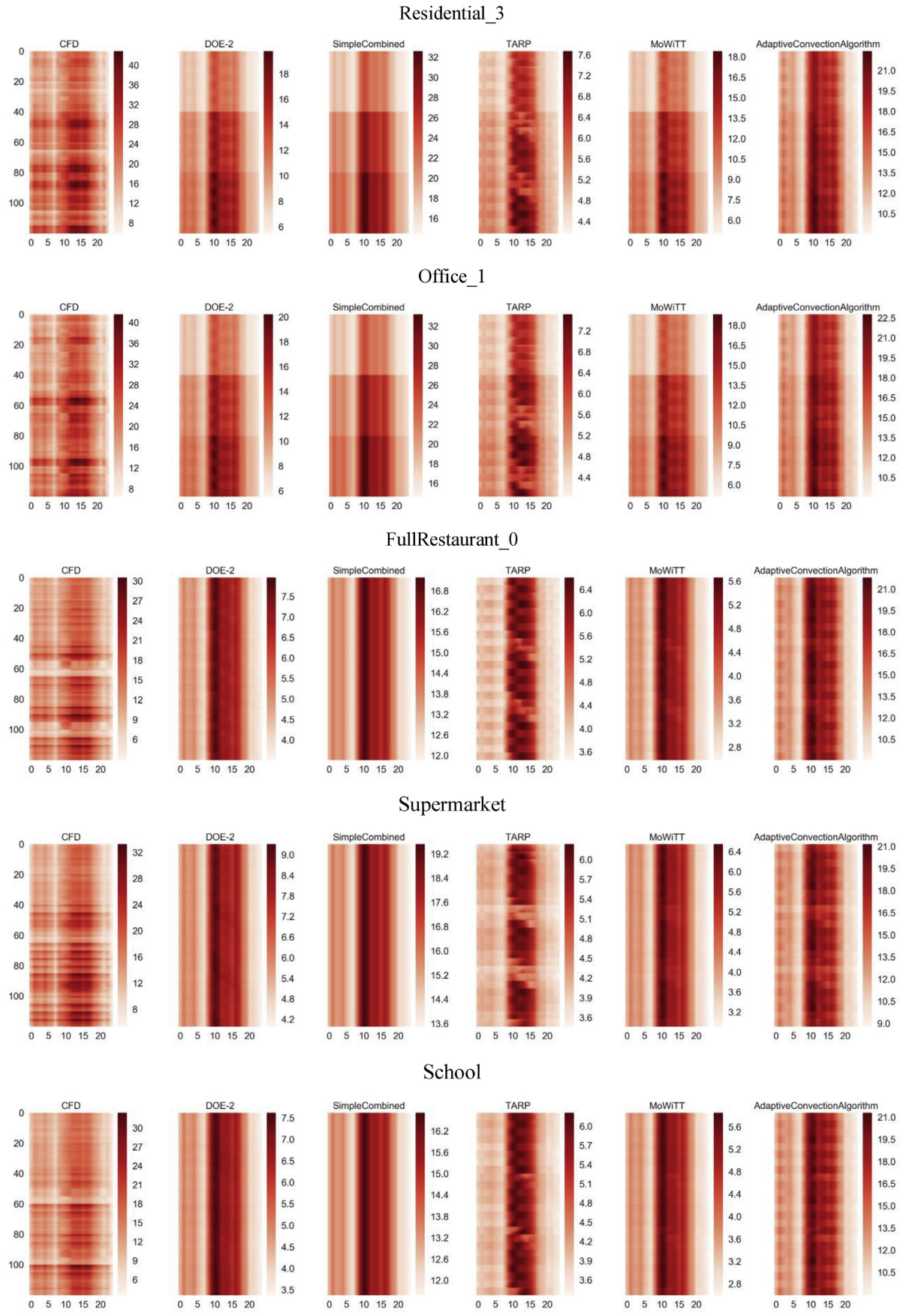

Fig. 7. Average CHTCs of different types of buildings in neighbourhood form scenarios (unit of color bar: W/m^{2}K). (For interpretation of the references to color in this figure legend, the reader is referred to the Web version of this article.)

floor building types in the neighbourhood such as restaurant buildings, supermarket, and school. The heatmaps of empirical algorithms does not manifest much difference in darkness along y-axis as they do for multi-floor buildings, which implies that for all of them, the multiplier does not exert impact on the calculation results of CHTC by the empirical methods. However, this is not true in practice. In terms of the heatmaps of the CFD method, the CHTCs are actually affected by the multipliers being applied to multi-floor buildings, implying that the wind speed around the single-floor buildings is influenced by the changes in the height of those multi-floor buildings. This is what is often called the skyscraper wind effect, which suggests more intense wind around the base of tall structures. Usually, accelerated wind can be caused by "downdraught effect", and the higher wind speed can lead to higher CHTC values compared to the values calculated by empirical methods since they do not consider the wind environment created by surrounding buildings. Hence, the multiplier does not only affect the CHTCs of multi-floor buildings, but also their surrounding buildings in the neighbourhood.

To further understand the effects of the neighbourhood form on CHTC, the visualization of the CFD simulation results are plotted in Fig. 8. The selected timestep to be visualized is 10 o'clock in the morning when the wind speed is 6.2 m/s and the wind direction is 310°. In Fig. 8, the CHTC on the building walls are compared with the three different multipliers. With the neighbourhood orientation being controlled at 135°, it can be observed that when the multiplier grows, the CHTC on the walls of the high-rises increases. Another important observation is that other than multiplier (building height), different setbacks also lead to different wind environment for the buildings and the change in CHTCs. The last plot in Fig. 8 shows the increase in building setback can cause different wind environment among buildings and results in overall lower CHTC values for the buildings in the neighbourhood.

5.2. Deviation in heating and cooling load calculations

To better analyze and compare the heating and cooling load results for the buildings in the neighbourhood, the metric similar to EUI — thermal load intensity (LI) is used, which is the heating or cooling load averaged by building conditioned floor area. The analysis in the following sections all refer to LI, which is thermal load per m^2 conditioned floor area.

The difference of hourly heating and cooling load simulated by using the proposed CFD method and the empirical methods are calculated and processed. The results are shown in Fig. 9. Buildings with similar error patterns are skipped in plotting, leaving one representative building for each type in the figure. The violin plots in Fig. 9 indicate the distribution of the LI errors brought by using different algorithms in calculating CHTCs. The errors are calculated by Equation (9).

$$\varepsilon_i = LI_{emp,i} - LI_{cfd,i} \tag{9}$$

where $LI_{emp,i}$ and $LI_{cfd,i}$ are the heating or cooling load intensity calculated by empirical methods and the proposed CFD method at timestep i, respectively, in kJ/m^2h, ε_i is the deviation of the calculation results at timestep i.

Since the calculated results of deviations were conducted for each neighbourhood scenario and have excluded the factors affecting the LI including the changes in solar irradiations caused by orientation change, the deviations of LI are solely caused by the differences in CHTCs of external walls.

For residential buildings, the deviations mostly occur for the hourly heating load intensity (HLI). Most of the empirical methods tend to underestimate HLI since they usually underestimate the CHTCs and a low CHTC can lead to lower heat flux to the outer environment. In this case, a lower heat flux means less heat loss to

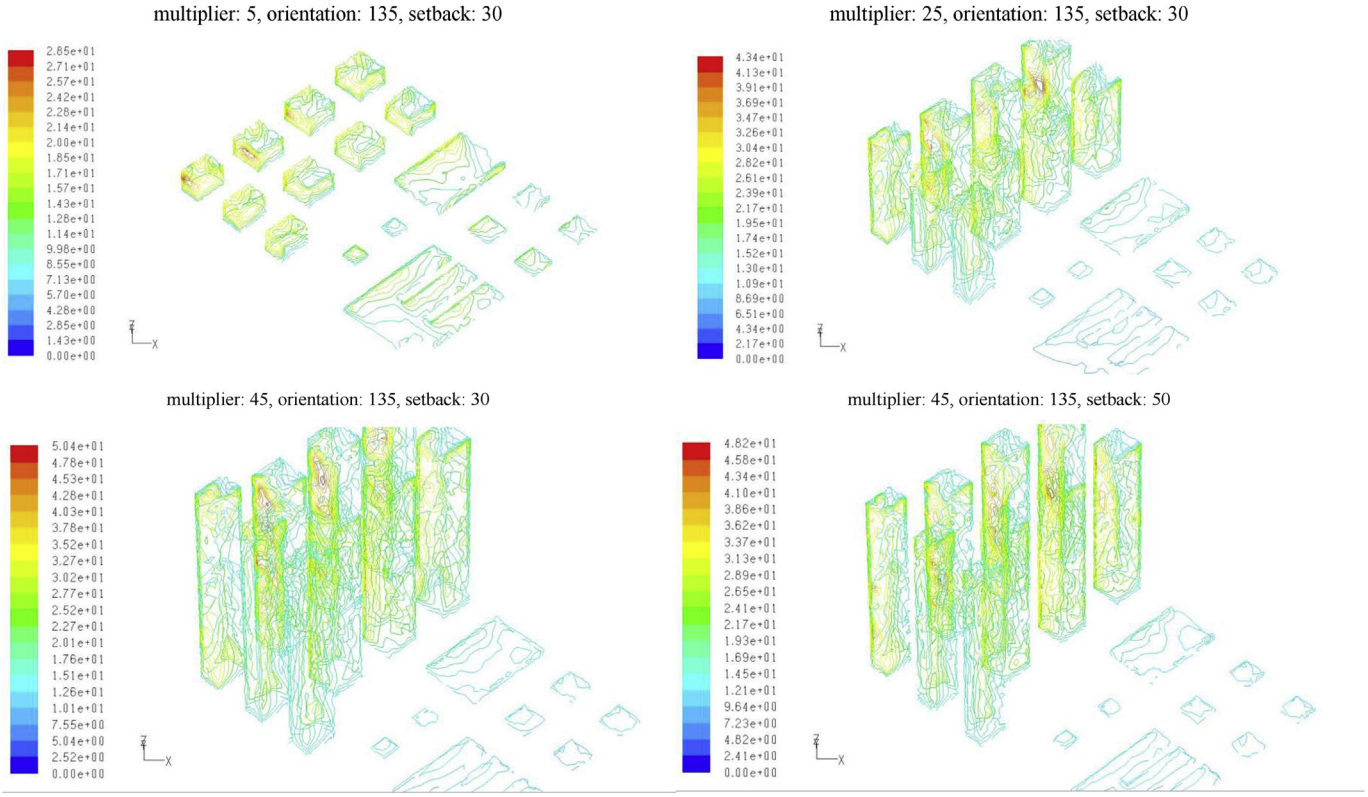

Fig. 8. Fluent simulation results of CHTCs for various multipliers and setbacks at 10 am.

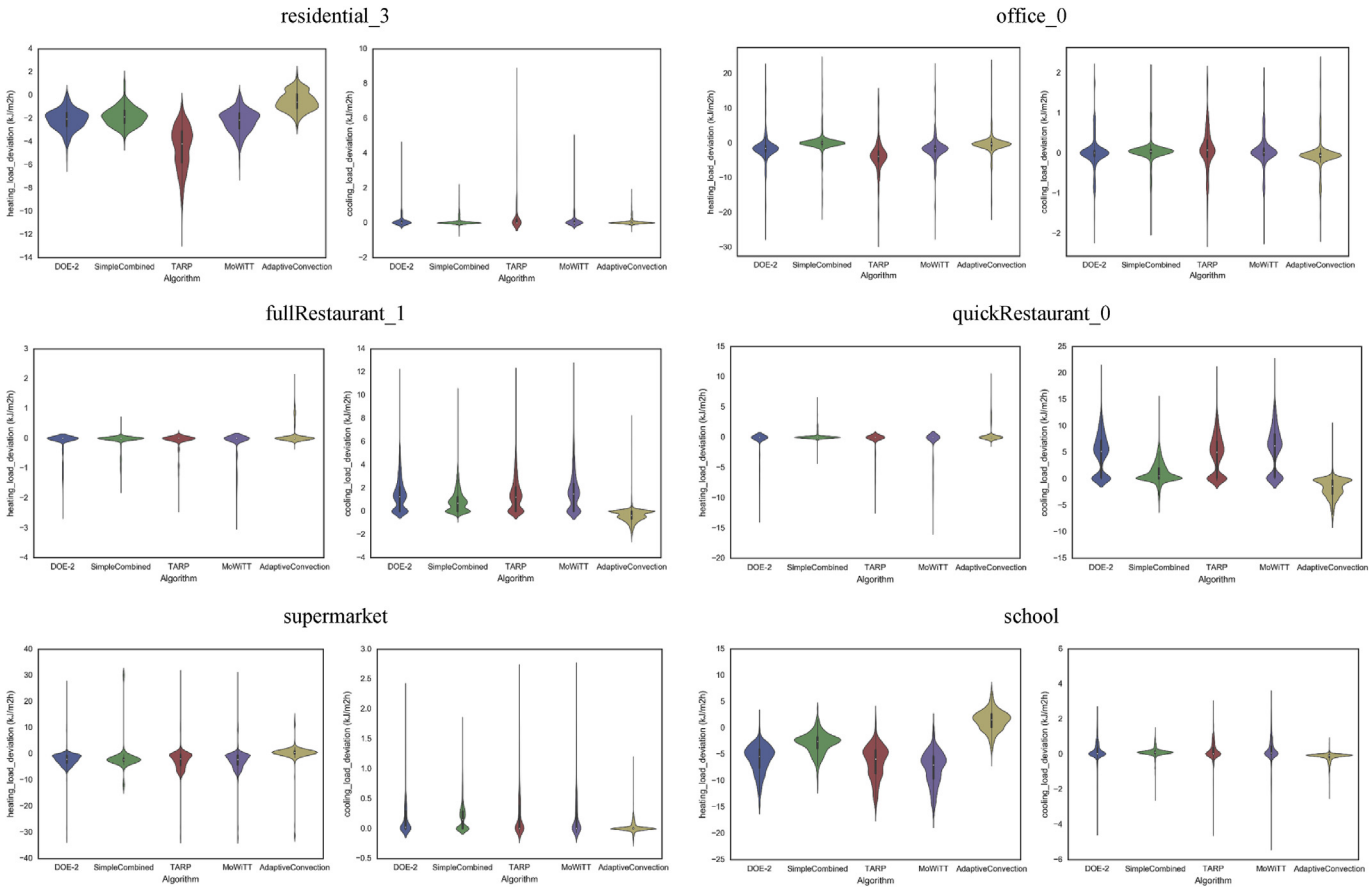

Fig. 9. Deviations of simulated heating and cooling load.

the cold outdoor environment. The AdaptiveConvection algorithm produces the least errors, and together with SimpleCombined algorithm, they sometimes overestimate the HLI. The deviation of the cooling load intensity (CLI) sometimes reaches 8 kJ/m^{2}h for some algorithms, but this situation rarely happens. For office building, the conclusion of the residential building's HLI also applies, but the magnitude of the deviation sometimes can reach ± 20 kJ/m^{2}h. For CLI, the deviation is less than HLI mainly because it is in winter and the office building itself is having small amount of cooling load.

For restaurants, the quick restaurant and the full restaurant share the similar pattern in the LI deviations. Using the proposed CFD method does not show much difference in predicting building heating load, while there are deviations in CLI. Considering that those types of buildings operate during day time and its internal load is high because of occupant behavior and routine cooking load, its thermal load is mainly cooling-load driven and not much heating is needed during the day. Therefore, in contrast to the residential buildings that are mainly heating-load driven, the simulation deviations between the coupled CFD method and the empirical methods mainly occur in cooling load prediction and most of the empirical methods tend to overestimate the cooling load.

For supermarket and school, both of the buildings have large conditioned floor area and similar thermal properties, but the deviations of CLI and HLI of the two buildings are different. For the supermarket, the deviation of CLI is small, and most of the time, there is no deviation between the coupled CFD method and the empirical methods in HLI prediction except that the deviation rarely reaches ± 30 kJ/m^{2}h, but the deviations of HLI for the school occur more in frequency. This is due to the fact that though these two buildings have similar floor area, the shape of the buildings are very different. The supermarket is large square shaped building with far fewer external structures exposed to the outer environment compared with the school. The shape of the school is shown in Fig. 4 and it has more external walls transferring heat flux between the indoor and outdoor environment. Therefore, the supermarket is more thermally isolated to the outdoor environment compared to the school. The cold winter in Chicago will make the school more likely to be affected by outdoor environment and thus creating deviations between different CHTC calculation methods.

The conclusion after analyzing the difference between the heating and cooling load results obtained by using the proposed method and the empirical methods could be drawn that during the winter time in Chicago, the effect of CHTCs on building's HLI is diminished when the building becomes more dominated by internal load, such as restaurant, supermarket, or office buildings with large internal load. For those types of buildings, the CFD coupling procedure does not help so much in obtaining a more reliable energy simulation result on building HLI. However, the deviation of CLI still suggests the use of CFD coupling procedure for the building simulation will make the CLI results more corresponding to the outdoor wind environment.

In Table 1, the percentage deviations of the summed daily HCI and CLI caused by using the proposed method and the empirical methods are summarized, and the deviations calculated for each individual building have been aggregated to six building types. The calculation of the percentage deviation of one type of building is described by Equation (10):

Table 1
Analysis of the deviations of daily HCI and CLI by different algorithms for the six building types.

		SimpleCombined	AdaptiveConvection	TARP	MoWiTT	DOE-2
fullRestaurant	max	3.24%	2.21%	3.36%	**3.80%**	0.36%
	mean	1.91%	1.13%	1.92%	**2.24%**	−0.51%
	min	0.31%	−0.25%	0.24%	0.51%	**−1.52%**
	std	0.57%	0.44%	0.63%	**0.69%**	0.31%
market	max	−1.03%	−0.70%	−0.89%	**−1.05%**	1.04%
	mean	−2.06%	−1.31%	**−2.28%**	−2.37%	0.20%
	min	−3.36%	−2.22%	−3.75%	**−4.03%**	−0.98%
	std	0.51%	0.40%	**0.69%**	0.64%	0.49%
office	max	1.08%	**3.18%**	−1.44%	0.61%	2.32%
	mean	−2.08%	−0.17%	**−4.50%**	−2.09%	−0.87%
	min	−5.03%	−3.13%	**−8.21%**	−4.99%	−4.28%
	std	1.11%	0.87%	**1.31%**	1.09%	0.99%
quickRestaurant	max	6.15%	3.18%	6.03%	**6.83%**	0.80%
	mean	3.83%	1.24%	3.74%	**4.43%**	−1.15%
	min	1.49%	−1.48%	1.17%	2.20%	**−4.14%**
	std	0.78%	0.69%	0.78%	**0.83%**	0.81%
residential	max	−0.34%	1.95%	−5.70%	−0.71%	**2.95%**
	mean	−4.29%	−3.56%	**−8.92%**	−4.52%	−1.15%
	min	−6.74%	−5.93%	**−14.61%**	−7.12%	−4.37%
	std	0.79%	1.38%	**1.61%**	0.83%	1.14%
school	max	−7.48%	0.00%	−8.90%	**−11.29%**	9.94%
	mean	−13.81%	−6.39%	−15.08%	**−17.58%**	3.14%
	min	−19.38%	−11.53%	−20.80%	**−23.21%**	−3.83%
	std	2.23%	2.12%	2.41%	2.46%	**2.50%**

$$\frac{\sum_i \left(CLI_{emp,i} + HLI_{emp,i}\right) - \sum_i \left(CLI_{cfd,i} + HLI_{ecfd,i}\right)}{\sum_i \left(CLI_{cfd,i} + HLI_{ecfd,i}\right)} \tag{10}$$

The presentation of the calculated percentage deviations is to show how the daily LI (sum of CLI and HLI) calculated by the empirical methods is going to be different from the proposed method. As shown in Table 1, the bold texts in the table shows the algorithm that has the largest deviation from the proposed method. According to the results, SimpleCombined and AdaptiveConvection algorithm have the best performance in predicting the sum of heating and cooling load. Comparatively AdaptiveConvection algorithm has the best performance in terms of the mean, max, min deviations of all the neighbourhood scenarios created by the 120 combinations of multipliers, orientations, and setbacks.

5.3. Heating and cooling load analysis

After comparing the deviations in calculating CLI and HLI between the empirical method and the proposed coupled CFD method, the results of CLI and HLI simulated by the proposed CFD coupled method are analyzed further to study how the neighbourhood form impacts the energy performance of the buildings in it. The violin plots of CLI and HLI for representative buildings of the six types are shown in Fig. 10. The y-axis in the figure is the daily aggregation of the sum of CLI and HLI under the 120 different neighbourhood forms in this research.

As shown in Fig. 10, the ranges of the building LI could be large under different forms of the neighbourhood. For residential and office buildings, the daily LI ranges from 900 kJ/m^{2}day to 1500 kJ/m^{2}day and from 1850 kJ/m^{2}day to 2500 kJ/m^{2}day, respectively. For full restaurants and quick restaurants, the range could be from 1450 kJ/m^{2}day to 1680 kJ/m^{2}day and from 2300 kJ/m^{2}day to 2650 kJ/m^{2}day, respectively. The ranges for the supermarket and the school are 2250 kJ/m^{2}day to 2480 kJ/m^{2}day and from 860 kJ/m^{2}day to 1110 kJ/m^{2}day, respectively. The individual buildings with the same type share the similar ranges but the exact distribution of LI may have small difference with each other in terms of their relative locations in the neighbourhood.

Table 2 summarizes important statistics of the LI ranges for each building. It shows that the maximum sum of cooling and heating load can be as much as 27.1% more than the average level for the residential buildings, and that value for the office buildings, full restaurants, quick restaurants, supermarket, and school, is 17.2%, 6.1%, 6.4%, 2.3%, and 12%, respectively. At the same time, the lowest thermal load scenario for each type of building can be −18.6% (residential), −7.7% (office), −4.7% (full restaurant), −4.3% (quick restaurant), −3.6% (supermarket), −7.5% (school), less than the average level. It is found that the neighbourhood form can have significant impact on the thermal load of the building during the winter in Chicago for the residential building and the school because they are more susceptible to outdoor environment. For other types of low-rise building that are more dominated by internal load compared with the residential building and the school, the impacts of the multiplier, orientation, and the setback of the neighbourhood on the LI are limited. Though office building is also internal load driven type, its heating and cooling load can be different as much as 17.2% mostly due to the increase in height introduces higher CHTC for the building external envelope and leads to more energy transfer with the outdoor environment.

5.4. Impacts of neighbourhood features on building thermal load

To study the impacts of the three neighbourhood features — multiplier, orientation, and setback on the building thermal load, the scatter plots of representative buildings for the six building types against the three features are plotted in Fig. 11 and Fig. 12. In Fig. 11, residential_0 and residential_5 are chosen to represent the residential buildings as they show two major groups of patterns in the scatter plot. The residential buildings in the first row has the pattern of residential_0 while the second row has the pattern of residential_5. For other types of buildings, each of them shares the similar pattern respectively.

As shown in Figs. 11 and 12, four types of buildings, including residential, office, supermarket, and school share similar response to the change in multiplier — the LI increases as the multiplier increases, which is due to that the augment in multiplier increases the CHTCs on a whole and the HLI will be on the rise. Whilst for

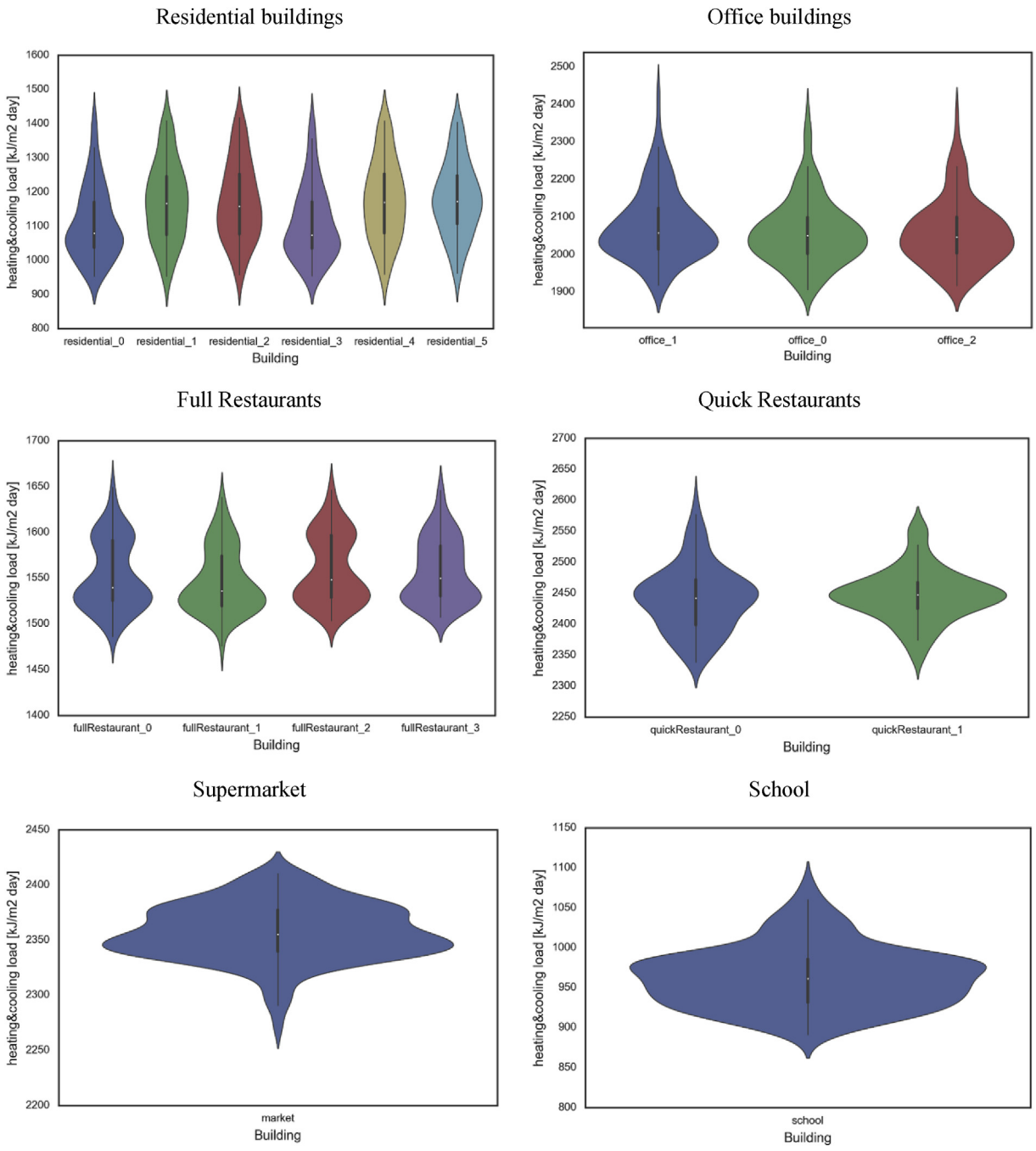

Fig. 10. Ranges of the sum of CLI and HLI for each building under different neighbourhood forms.

restaurants, their LIs is reduced as the multiplier increases. As discussed in the previous sections, the LI of restaurants is mainly driven by cooling load, and the increase in CHTCs in the winter can actually reduce the total LI. Another important factor is the solar radiation. When the multiplier increases, the high-rises provide shades for the building in the area, and the lowered solar radiation in the area further increases LI for heating-load driven buildings and decreases LI for cooling-load driven buildings.

The responses of the buildings to the changes in orientation differ from one another. A further insightful observation of the scatter plot implies the CHTCs can be low on average from the range of 135–225° because residential, office, supermarket, and school show lower LI and the restaurants show relatively higher LI inside this range. To benefit most of the buildings in the neighbourhood energy-wisely, the orientation of the neighbourhood should be chosen between 135 and 225° relative to the north. The solar radiation also benefits the low-rise buildings located on the south side of the neighbourhood under this range of orientations in the winter. 180° would be a good selection for the neighbourhood according to the analysis results.

For residential, office, supermarket, and school, the LI decreases when the setback among buildings is enlarged, while for restaurants, the LI increases on the contrary, which implies that increasing the setback results in lower heating load and potentially higher cooling load. A larger setback allows sunlight into the neighbourhood and benefits the LI level for heating-load driven

Table 2
Summary of LI ranges for each building (unit: kJ/m^2 day).

	mean	median	standard deviation	(max-mean)/mean (%)	(min-mean)/mean (%)
fullRestaurant_0	1554.08	1540.55	36.82	6.13	−4.37
fullRestaurant_1	1547.33	1536.61	34.50	5.88	−4.63
fullRestaurant_2	1561.59	1549.96	36.67	5.41	−3.73
fullRestaurant_3	1558.48	1555.33	34.65	5.60	−3.30
supermarket	2356.91	2354.69	25.83	2.25	−3.61
office_0	2057.51	2047.35	88.28	15.24	−7.50
office_1	2073.97	2054.44	94.13	17.21	−7.65
office_2	2056.61	2043.88	88.71	15.43	−6.93
quickRestaurant_0	2442.35	2442.59	52.73	6.36	−4.26
quickRestaurant_1	2446.79	2447.23	42.53	4.50	−4.23
residential_0	1108.74	1079.34	106.35	27.09	−13.96
residential_1	1172.38	1166.33	115.34	20.13	−18.62
residential_2	1171.17	1157.47	115.42	21.08	−18.22
residential_3	1109.55	1073.96	107.57	26.59	−13.92
residential_4	1177.19	1169.81	117.37	19.56	−18.48
residential_5	1179.57	1172.16	108.07	19.03	−18.45
school	962.98	961.31	38.54	11.97	−7.46

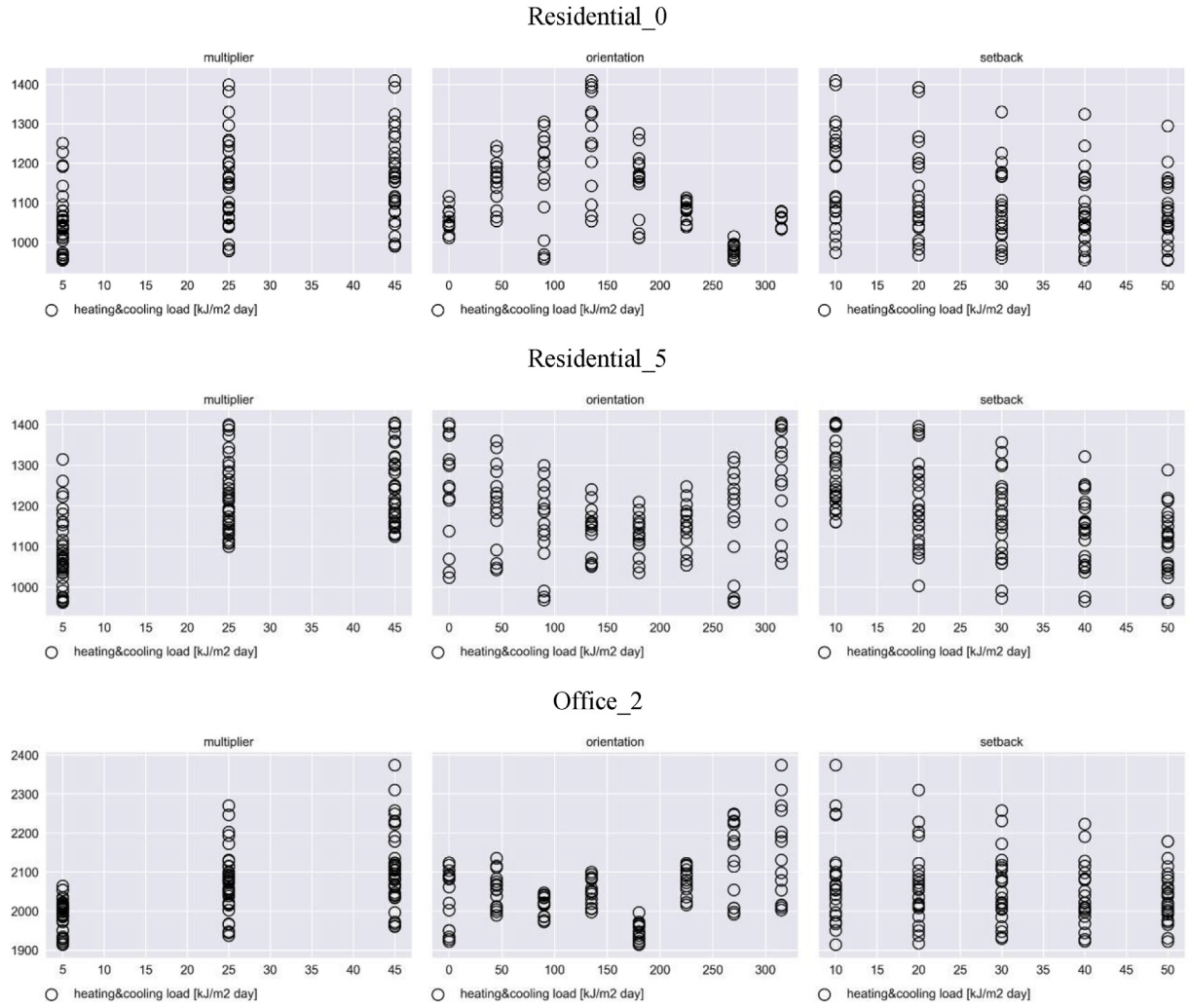

Fig. 11. Scatter plot of high-rise building thermal load against each neighbourhood feature.

buildings in the area.

To conclude, the simulation results and analysis lead to a design guideline for the optimal energy performance of the buildings in the neighbourhood: low multiplier — decreasing building heights for multi-floor buildings like residential and office buildings; an orientation of 135–225° relative to the north — putting comparatively higher buildings on the north side of the neighbourhood; and a larger setback — increasing the spaces among buildings in the

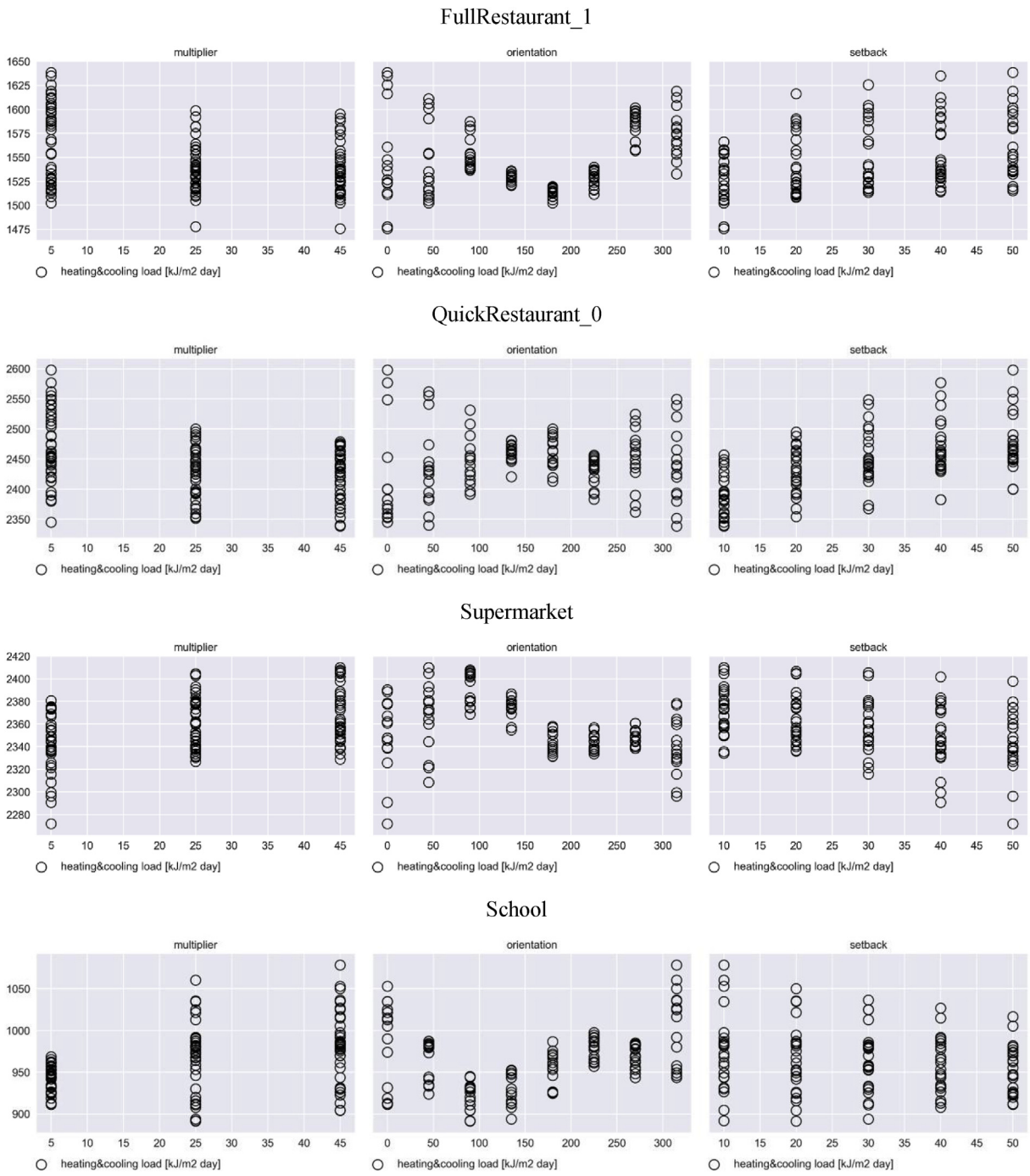

Fig. 12. Scatter plot of low-rise building thermal load against each neighbourhood feature.

neighbourhood to allow more sunlight land on the building surfaces.

5.5. Feature importance

As shown in Figs. 11 and 12, the relationship between the building thermal load and the neighbourhood features cannot be linear because the orientation feature introduces non-linear correlations. Therefore, linear regression is not suitable in this case to find the importance of each feature on the building thermal load. In this research, decision tree (DT) is used to find the relative influences of each feature on the LI. DT is method that makes use of graph or tree model to learn and predict the schema of the best routes or rules. It can be both used to perform classification or regression tasks. It is the set of assumptions that the learner uses to predict outputs given inputs that it has not encountered [43]. One of the widely used DT algorithms is the top-down induction of decision trees (ID3, C4.5 by Quinlan) [44]. In this research, there is no outlier in the training database and what is needed from this algorithm is to let it fit all the data points in order to find the influential features. For the DT, there is an important property called “feature importance” in the final trained model, which is used to determine the importance of each feature in making the rule-based decisions. Literature [44] can be referred regarding the

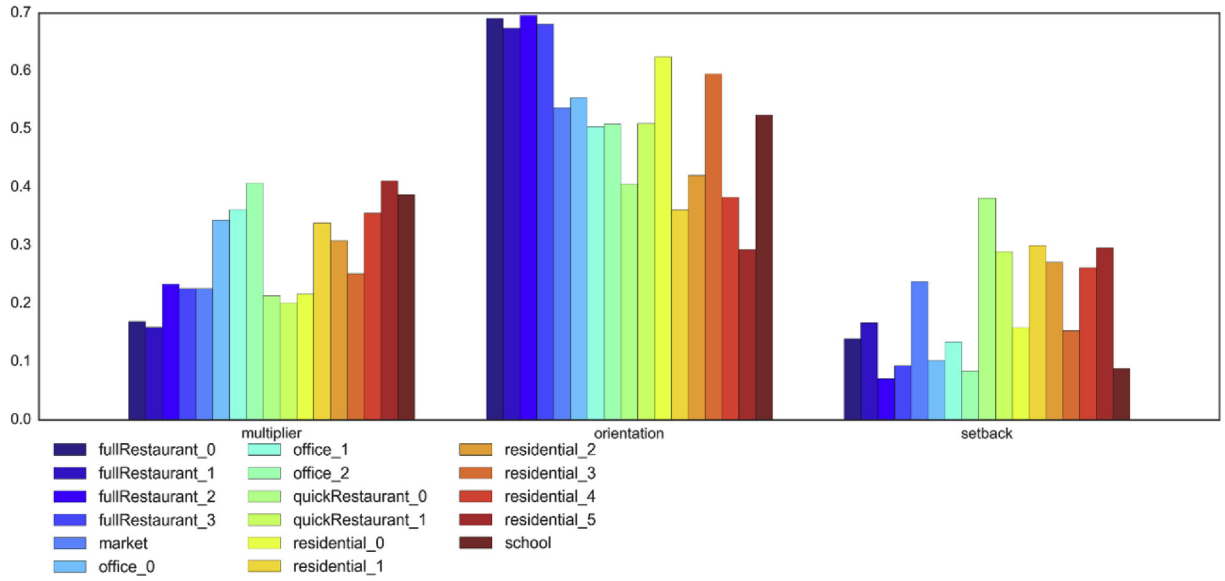

Fig. 13. Importance of the neighbourhood features.

details of the algorithm and it won't be introduced in detail in this paper.

For each building, the training features include the 120 combinations of multiplier, orientation, and setback, and the training target is the building total thermal load intensity. After processing the feature importance of the trained regression model of each building, the results are visualized in Fig. 13.

As shown in Fig. 13, the feature importance varies from building to building, but generally, orientation is the feature that has the most impact on the buildings LI, especially for restaurants. For residential and office buildings, the multiplier and the orientation have the same impacts on the building LI. Neighbourhood setback has the least influences on the building LI, but it still cannot be ignored in the design of the neighbourhood. According to the results in Fig. 13, it is suggested that the changes in solar radiation and the local wind environment brought by the orientation and multiplier are very influential to the building thermal load intensity and should be given more attention during the design process.

6. Conclusions

In this research, a neighbourhood-scale CFD coupled energy simulation framework has been proposed and developed. The BCVTB is used to dynamically couple the CHTC calculation results generated by CFD simulation at each timestep to the building energy simulation in EnergyPlus. Arrays of buildings of six different types are set up inside a neighbourhood. Three neighbourhood features — multiplier, orientation, and setback, are used to alter and manipulate the neighbourhood form in order to find the impacts of these features on building thermal load intensity in Chicago's windy winter.

The five EnergyPlus built-in empirical methods in calculating CHTCs have been compared with the proposed coupled CFD method, and the differences among them are analyzed. It is found that the CHTCs calculated by the AdaptiveConvection and the SimpleCombined algorithms are closest to the proposed method. In addition, the two algorithms also have the best performance in predicting the total value of heating and cooling load.

In terms of building thermal performance, it can be found that in the winter, both the LI deviations of the empirical methods from the proposed CFD method and the impacts of neighbourhood forms on building LI are more significant for heating-load driven building types such as residential buildings or school and are less significant for cooling-load driven building types such as restaurants and supermarket. For example, The LI results simulated by the proposed method show that the maximum sum of cooling and heating load can be as much as 27.1% more than the average level and −18.6% less than the average level for the residential buildings, and the values for the office buildings are +17.2% and −7.7%. Another important finding is that the simulation results and analysis can be used to find a design guideline for the optimal energy performance of the buildings in the neighbourhood in the winter: low multiplier, an orientation of 135–225° relative to the north, and a larger setback. Among the three neighbourhood features, the orientation has the biggest influence on the building thermal performance, and the multiplier follows. Setback also have its influence, but it is relatively limited.

The proposed method and framework can be applied to the study in various places and climates, and Chicago is used as a case study in this research. The computational resources could be high in coupling the CFD to energy simulation, but with the future cloud computation technology, the computational time for this kind of research is affordable. The limitations of the research lie in that more complicated neighbourhood forms exist and that the urban microclimate is not considered as the boundary for the neighbourhood. Nevertheless, the framework proposed in this research can be an important procedure or method in future studies considering the above limitations.

Acknowledgement

This work was supported in part by the National Key R&D Program of China (No. 2017YFC0702300, 2017YFC0702306).

References

[1] Lee B, Hussain M, Soliman B. A method for the assessment of the wind-induced natural ventilation forces acting on low rise building arrays. Build Serv Eng Technol 1980;1(1):35–48.
[2] Hussain M, Lee B. A wind tunnel study of the mean pressure forces acting on large groups of low-rise buildings. J Wind Eng Ind Aerod 1980;6(3–4):207–25.

[3] Bauman F, Ernest D, Arens EA. The effects of surrounding buildings on wind pressure distributions and natural ventilation in long building rows. 1988.
[4] Shishegar N. Street design and urban microclimate: analyzing the effects of street geometryand orientation on airflow and solar access in urban canyons. J Clean Energy Technol 2013;1(1).
[5] Eliasson IÈ. The use of climate knowledge in urban planning. Landsc Urban Plann 1999;48(2000):31–44.
[6] Santamouris M, Papanikolaou N, Livada I, Koronakis I, Georgakis C, Argiriou A, et al. On the impact of urban climate on the energy consumption of buildings. Sol Energy 2001;70(3):201–16.
[7] Ramponi R, Blocken B, de Coo LB, Janssen WD. CFD simulation of outdoor ventilation of generic urban configurations with different urban densities and equal and unequal street widths. Build Environ 2015;92:152–66.
[8] Allegrini J, Carmeliet J. Simulations of local heat islands in Zürich with coupled CFD and building energy models. Urban Clim 2018;24:340–59.
[9] Allegrini J, Carmeliet J. Coupled CFD and building energy simulations for studying the impacts of building height topology and buoyancy on local urban microclimates. Urban Clim 2017;21:278–305.
[10] Beausoleil-Morrison I, Clarke J, Denev J, Macdonald I, Melikov A, Stankov P. Further developments in the conflation of CFD and building simulation. 2001.
[11] Bartak M, Beausoleil-Morrison I, Clarke JA, Denev J, Drkal F, Lain M, et al. Integrating CFD and building simulation. Build Environ 2002;37(8):865–71.
[12] Hand JW. The ESP-r cookbook. Glasgow, Scotland: University of Strathclyde; 2011.
[13] Allegrini J, Dorer V, Carmeliet J. Analysis of convective heat transfer at building façades in street canyons and its influence on the predictions of space cooling demand in buildings. J Wind Eng Ind Aerod 2012;104–106:464–73.
[14] Liu J, Heidarinejad M, Gracik S, Srebric J, Yu N. An indirect validation of convective heat transfer coefficients (CHTCs) for external building surfaces in an actual urban environment. Build Simulat 2015;8(3):337–52.
[15] Liu J, Srebric J, Yu N. Numerical simulation of convective heat transfer coefficients at the external surfaces of building arrays immersed in a turbulent boundary layer. Int J Heat Mass Transf 2013;61:209–25.
[16] Emmel MG, Abadie MO, Mendes N. New external convective heat transfer coefficient correlations for isolated low-rise buildings. Energy Build 2007;39(3):335–42.
[17] Blocken B, Defraeye T, Derome D, Carmeliet J. High-resolution CFD simulations for forced convective heat transfer coefficients at the facade of a low-rise building. Build Environ 2009;44(12):2396–412.
[18] Defraeye T, Blocken B, Carmeliet J. CFD analysis of convective heat transfer at the surfaces of a cube immersed in a turbulent boundary layer. Int J Heat Mass Transf 2010;53(1):297–308.
[19] Liu J, Heidarinejad M, Gracik S, Srebric J. The impact of exterior surface convective heat transfer coefficients on the building energy consumption in urban neighborhoods with different plan area densities. Energy Build 2015;86:449–63.
[20] Mirsadeghi M, Cóstola D, Blocken B, Hensen JLM. Review of external convective heat transfer coefficient models in building energy simulation programs: implementation and uncertainty. Appl Therm Eng 2013;56(1):134–51.
[21] Yi YK, Feng N. Dynamic integration between building energy simulation (BES) and computational fluid dynamics (CFD) simulation for building exterior surface. Build Simulat 2013;6(3):297–308.
[22] Zhang R, Lam KP, Yao S-c, Zhang Y. Coupled EnergyPlus and computational fluid dynamics simulation for natural ventilation. Build Environ 2013;68:100–13.
[23] Zhai Z, Chen Q, Haves P, Klems JH. On approaches to couple energy simulation and computational fluid dynamics programs. Build Environ 2002;37(8):857–64.
[24] Negrao. Conflation of computational fluid dynamics and building thermal simulation. Glasgow, Scotland: University of Strathclyde; 1995.
[25] Srebric J, Chen Q, Glicksman LR. A coupled airflow and energy simulation program for indoor thermal environmental studies. Cambridge, MA (US): Massachusetts Inst. of Tech.; 2000.
[26] Wang L, Wong NH. Coupled simulations for naturally ventilated residential buildings. Autom ConStruct 2008;17(4):386–98.
[27] Negrão COR. Conflation of computational fluid dynamics and building thermal simulation. 1995.
[28] Srebric J, Chen Q, Glicksman LR. A coupled airflow and energy simulation program for indoor thermal environmental studies. 2000.
[29] Goel S, Athalye RA, Wang W. Enhancements to ASHRAE standard 90.1 prototype building models. Richland, WA (United States): Pacific Northwest National Lab. (PNNL); 2014.
[30] Quan SJ, Economou A, Grasl T, Yang PP-J. Computing energy performance of building density, shape and typology in urban context. Energy Proc 2014;61:1602–5.
[31] Wilcox S, Marion S. Users manual for TMY3 data sets. Golden, CO: National Renewable Energy Laboratory; 2008. NREL/TP-581-43156.
[32] Deru M, Field K, Studer D, Benne K, Griffith B, Torcellini P, Liu B, Halverson M, Winiarski D, Rosenberg M, Yazdanian M, Huang J, Crawley DUS. Department of Energy commercial reference building models of the national building stock. 2011. p. 1–118. DOE, http://digitalscholarship.unlv.edu/renew_pubs/44.
[33] ASHRAE. ANSI/ASHRAE/IESNA Standard 90.1-2016. Energy standard for buildings except low-rise residential buildings. Rocky Mountain; 2016.
[34] Standard A, Chapter RM. ANSI/ASHRAE/IESNA Standard 90.1-2004. Energy standard for buildings except low-rise residential buildings. 2004.
[35] Beausoleil-Morrison I. The adaptive coupling of heat and air flow modelling within dynamic whole-building simulation. Citeseer; 2000.
[36] DOE. The EnergyPlus engineering reference. 8.0 ed. EnergyPlus Development Team; 2015.. http://www.energyplus.gov.
[37] ASHRAE. ASHRAE Handbook e Fundamentals. 1981. Atlanta, GA1981.
[38] EnergyPlus. EnergyPlus engineering reference – the reference to EnergyPlus calculations. DOE; 2007.
[39] Yazdanian M, Klems J. Measurement of the exterior convective film coefficient for windows in low-rise buildings. 1993.
[40] Handbook A. Fundamentals. American society of heating, refrigerating and air conditioning Engineers, Atlanta. 2001. p. 111.
[41] Brooks C, Lee EA, Liu X, Zhao Y, Zheng H, Bhattacharyya SS, et al. Ptolemy II-heterogeneous concurrent modeling and design in Java. 2005.
[42] Wetter M. Co-simulation of building energy and control systems with the building controls virtual test bed. J Build Perform Simulat 2011;4(3):185–203.
[43] Mitchell TM. The need for biases in learning generalizations. New Brunswick, New Jersey, USA: Rutgers University; 1980. CBM-TR 5-110.
[44] Quinlan JR. Induction of decision trees. Mach Learn 1986;1(1):81–106.